Gas-Liquid Agitation with Closed Turbine Type Impellers Modified for Blade Geometries



M. Yoshida,* M. Nakata, K. Itagaki, K. Suganuma, R. Kiyota, S. Kogami, and Y. Takahashi

Department of Applied Sciences

Department of Applied Sciences, Muroran Institute of Technology, 27-1, Mizumotocho, Muroran 050-8585, Japan doi: https://doi.org/10.15255/CABEQ.2025.2426

Original scientific paper Received: April 25, 2025 Accepted: October 15, 2025

An agitation impeller with shrouded blades—specifically, a closed impeller—was redesigned. A closed impeller originating from a conventional turbine-type impeller was analyzed by considering the internal liquid flow characteristics. As a result, an impeller consisting of six flat blades with radially tapered widths was developed for closed-mode operation. The modified closed impeller (6RTW-FCI) was applied to gas-liquid agitation. The flow behavior of the gas-liquid mixture in the impeller region was examined with energy considerations based on the impeller power characteristics in the gassed liquid. The internal cavities of the 6RTW-FCI generated gas bubbles that moved radially outward due to the accelerated liquid flow produced by the impeller. The power characteristics of the 6RTW-FCI in terms of relative power consumption, which was with no sudden change for various aeration-agitation rates, supported energy conversion through the impeller, resulting in favorable gas-liquid dispersion.

Keywords

agitation vessel, closed impeller, blade geometries, gas-liquid dispersion, power characteristics

Introduction

Bioprocesses for the production of valuable bioproducts may involve the aerobic liquid culture of microorganisms such as yeast, bacteria, and cells on microcarriers. These culture operations are typically carried out in vessels agitated by mechanically-driven rotating impellers. Impeller design plays a crucial role in achieving effective liquid-phase mixing and enhancing heat and mass transfer in gas-liquid agitation vessels^{1,2}. The impeller standardly employed in bioreactors of this type is a disk turbine impeller with six flat blades (6STD impeller)^{3,4}. The 6STD impeller is preferred because it produces intense turbulence and thereby achieves effective gas-liquid dispersion^{3,5}. However, the 6STD impeller also exhibits conflicting characteristics associated with trailing vortices, which are attributable to the blade geometry^{6,7}. In vessels agitated by the 6STD impeller, a significant portion of the input energy is dissipated within the impeller rotation region, generating higher shearing action and resulting in nonuniform mixing throughout the vessel. Although such impeller action promotes gas-liquid mass transfer, it can also have an undesirable effect

on the microorganisms or cells^{8,9}. This may cause irreversible and morphological changes in the living bodies leading to cell rupture and death. Therefore, the design of agitation-type bioreactors should carefully consider the shearing action of the impeller^{10–14}.

In our previous work, we proposed an agitation impeller design that involved structural modification of a conventional turbine-type impeller¹⁵. The design concept aimed for the impeller blades to transmit energy to the liquid more efficiently while reducing dissipation in the impeller rotation region. This impeller, equipped with shrouds, was termed a "closed turbine-type impeller (6STD-FCI)" in contrast to the conventional "open turbine-type impeller (6STD-OI)". The 6STD-FCI was reported to generate internal liquid flow conducive to more effective energy transmission. The discharge flow of the 6STD-FCI, attributed to the shrouded blades, is characterized by the absence of trailing vortices. Focusing on these features, the closed impeller was applied to gas-liquid agitation¹⁶. The formation of gas cavities and their subsequent dispersion as gas bubbles using the 6STD-FCI, differed from those observed using the 6STD-OI. The differences in flow behavior of the gas-liquid mixture were reflected in the power characteristics of the impeller. A closed impeller is thus expected to reduce the shearing action of the impeller in the development

^{*}Corresponding author: Masanori Yoshida, E-mail: myoshida@mmm.muroran-it.ac.jp

of agitation-type bioreactors. However, the blade geometries have not been optimized for operation in the closed mode. Therefore, a rational approach in this regard should be to review the impeller design as an original for a closed impeller.

In this study, a modification of the closed impeller was attempted with the objective of rationalizing the impeller design. The dimensions of the flow path between neighboring blades were considered on the basis of the patterns of the internal liquid flows of the impellers. Agitating the liquid during gas sparging with a closed impeller, visual observations were performed in the region of impeller rotation. The impeller power consumption in the gassed liquid was measured to evaluate its characteristics in relation to gas-liquid dispersion.

Experimental

Experiments were conducted in a fully baffled, cylindrical vessel with a flat base made of transparent acrylic resin (300 mm inner diameter, D.). The liquid depth was maintained at D: 300 mm. Different designs of closed impellers and an open impeller (150 mm = $0.5D_t$ outer diameter, D_i), as described further herein, were set at a height of D/2from the vessel bottom. These impeller-to-vessel geometric conditions were adopted for the visualization and measurement of the liquid flow and the observation of the gas behavior¹⁶. The impeller rotation rate, $N_{\rm r}$, was adjusted to 100 rpm. The liquid phase was water (density, ρ , of 997 kg m⁻³ and viscosity of 0.890 mPa s), resulting in an impeller Reynolds number of 42000. Thus, the liquid flow within the vessels agitated by the impellers was determined as turbulent.

Tomographic visualization of the internal liquid flow of the impeller was performed on various horizontal planes in the impeller rotation region within the vessel, using the particle suspension method. Flow velocities were measured using two-dimensional particle tracking velocimetry (PTV). The details of the flow visualization and measurement were presented in the previous paper¹⁵. Based on continuous images acquired by video camera with a frame rate of 1000 fps, the velocity vectors for the predetermined positions were temporally averaged to yield mean velocities of the turbulent flows. The velocity components were divided into the circumferential and radial components, v_{θ} and v_{r} , respectively, to analyze internal liquid flow patterns.

To conduct gas-liquid agitation, the experimental vessel was equipped with a gassing system. A single-hole nozzle with a 5.0 mm inner diameter was used for air sparging.

Gas behavior during sparging into the liquid within the vessel was observed from the vessel bottom¹⁶. Impellers $(D_i = 150 \text{ mm} = 0.5D_t)$ were positioned at D/2 above the vessel bottom and rotated at $N_r = 100$ rpm under the condition of gassing at a volumetric gas flow rate, Q, of 20 L min⁻¹, corresponding to a superficial gas velocity, V_s , of 0.47 cm s⁻¹. The conditions for the impeller to capture the sparged gas and to generate gas bubbles were recorded using a video camera. For the examination of the impeller power characteristics, impellers with $D_i = 120 \text{ mm} = 0.4D_t \text{ were positioned at } D_t/3 \text{ above}$ the vessel bottom, representing practical impeller-to-vessel geometric conditions. Then, N was varied from 100 to 300 rpm. In combination, Q was varied from 10 to 100 L min⁻¹ for V_s of 0.24–2.36 cm s⁻¹. The impeller power consumption was determined by torque measurement using strain gauges attached to the shaft, while gas bubble dispersion in the bulk liquid was recorded simultaneously from the front by video camera.

Results and discussion

Modification of the closed impeller

In our previous work¹⁵, an impeller for liquid-phase agitation was prototyped by structurally modifying a conventional and standard disk turbine impeller with six flat blades (6STD). The modified impeller featured full shrouds (doughnut-shaped circular disks) on both the upper and lower sides of the blades, and was designated the "fully closed impeller (FCI)", whereas the original type was referred to as the "open impeller (OI)". The purpose of this design was to guide the liquid flow along the blade surfaces so that nearly all liquid entering the impeller could receive energy efficiently from the blades. Evaluation of the impeller characteristics in terms of hydraulic and energy efficiencies demonstrated the potential of the closed impeller for improved power transmission and more uniform power dissipation. However, internal liquid flow visualization of the 6STD-FCI, revealed a stagnant region near the rear of the blades, likely caused by flow separation on the blade surface (Fig. 1(a)). In the figure, the rotation direction is counter-clockwise and the right and left blade surfaces in the test area correspond to the front and rear sides, respectively. Such a flow field facilitated the formation of a secondary circulation within the passage between neighboring blades^{17–21}, which likely reduced impeller efficiency. In view of this, modification of the closed impeller was considered toward preventing the separation of the flow on the blade rear near the impeller disk.

The flow separation on the blade surface, as shown in Fig. 1(a), is presumed to result from insuf-

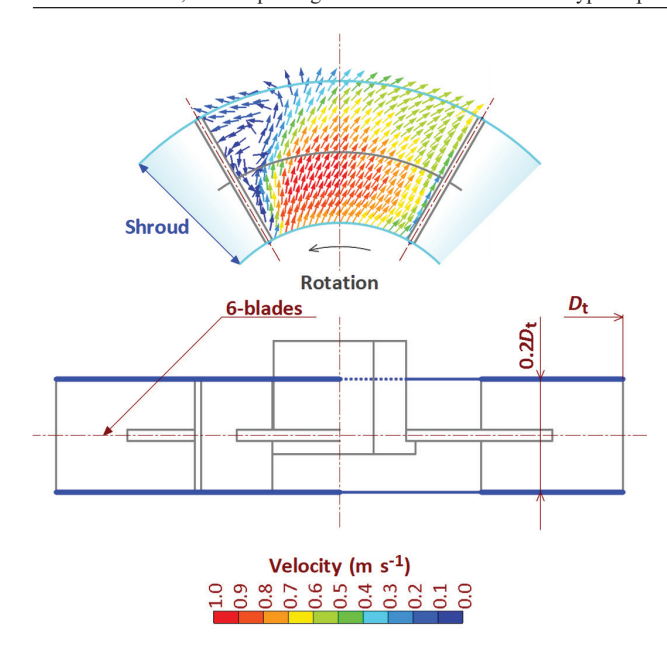


Fig. 1 (a) – 6STD-FCI design and liquid flow velocity profiles in its rotation region

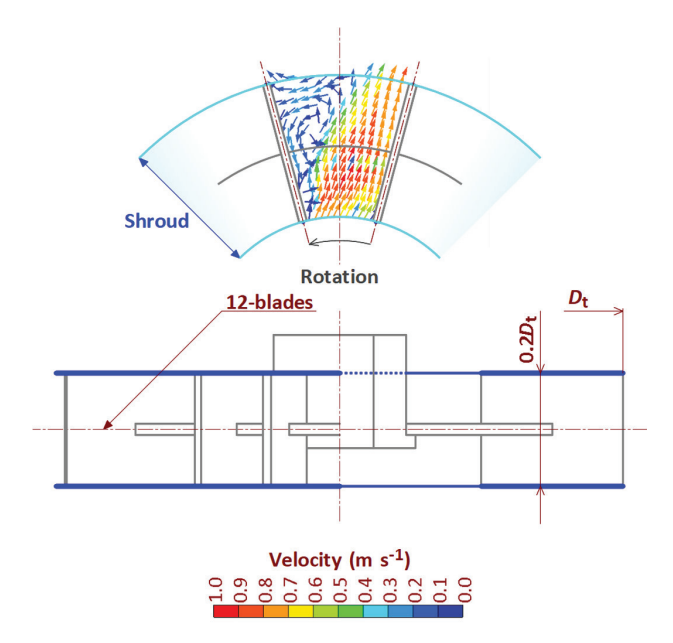


Fig. 1 (b) – 12STD-FCI design and liquid flow velocity profiles in its rotation region

ficient inflow in the impeller rotation region. When the fluid lacks sufficient kinetic energy to maintain continuous motion along the blade surface, flow separation occurs²². The inflow can generally be enhanced with an increase in impeller rotation speed, but the improvement may be limited depending on blade geometry^{23,24}. In this study, the design focused on adjusting the flow-path volume between adjacent blades to develop geometries suitable for closed-mode operation. Figs. 1(b), (c), and (d) show the modified impeller designs. The impeller with 12 flat blades of standard width (12STD) and the impeller with 6 flat blades of vertically small width

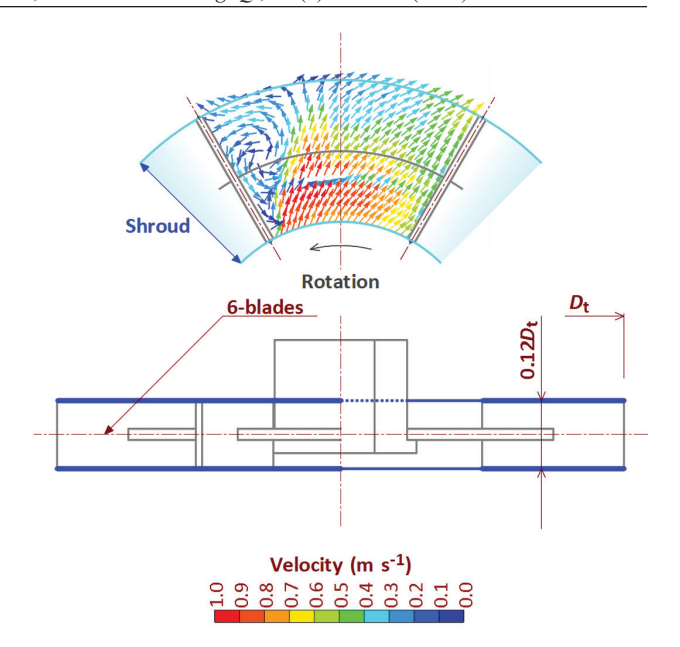


Fig. 1 (c) – 6VSW-FCI design and liquid flow velocity profiles in its rotation region

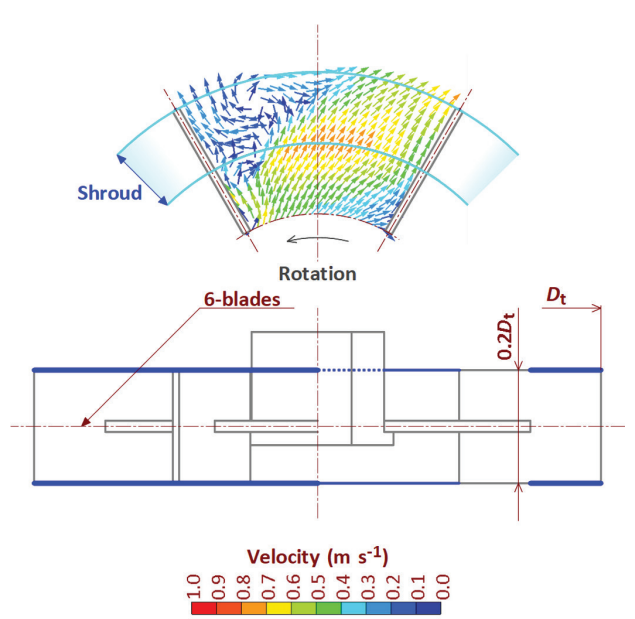


Fig. 1 (d) – 6STD-PCI design and liquid flow velocity profiles in its rotation region

(6VSW) provided narrower flow paths, reduced in the respective circumferential and axial directions. These impellers were used in closed mode. In the radial direction, the region shrouded by the doughnut-shaped circular disks was reduced, and the standard open impeller (6STD) was partially closed. Fully and partially closed impellers were abbreviated as FCI and PCI, respectively.

Internal liquid flows of modified closed impellers

The internal liquid flows of the modified closed impellers were examined. The circumferential and

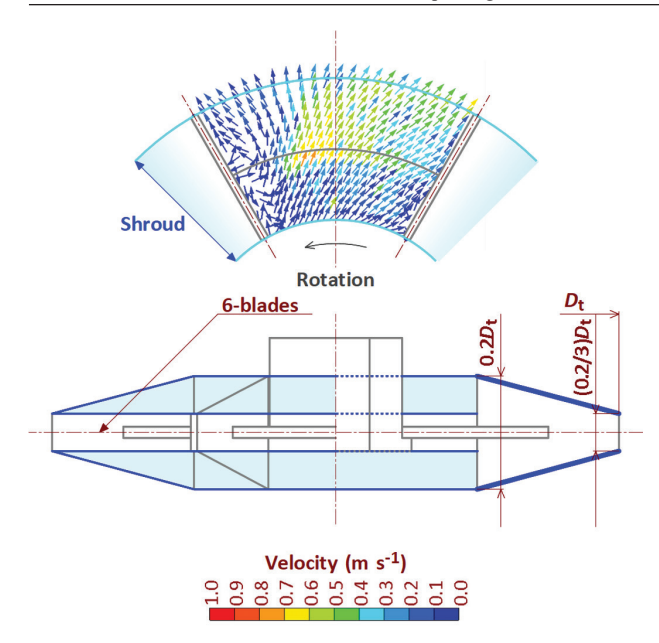


Fig. 1 (e) – 6RTW-FCI design and liquid flow velocity profiles in its rotation region

radial flow velocities, $v_{\rm A}$ and $v_{\rm r}$, were plotted against the radial position, as shown in Fig. 2(a) and (b), respectively. The velocities, averaged in the circumferential and axial directions, represent the overall flow field. For v_{a} , related to the head characteristics, the values for the radial positions of 12STD-FCI and 6VSW-FCI were slightly higher than those for 6STD-FCI. In contrast, the v_r values, associated with radial flow characteristics, were rather small for both 12STD-FCI and 6VSW-FCI. As shown in Figs. 1 (b) and (c), stagnant regions remained on the rear of the blades close to the impeller disk. Meanwhile, 6STD-PCI exhibited higher v_{a} and lower v_{a} values compared with 6STD-FCI, although a stagnant region was observed on a plane axially distant from the impeller disk (Fig. 1(d)). These results suggest that the increase in radial inertia associated with increased v possibly leads to an improvement in the internal flow following the impeller blades. However, as seen in Fig. 2(b), the radial flows of these closed impellers tend to decelerate radially and form an adverse pressure gradient, which is disadvantageous for the maintenance of the flow along the blade surface without flow separation²².

Development of closed impeller targeting radial flow

To address this, a new closed impeller design was developed, as shown in Fig. 1(e). This original impeller, designated 6RTW, featured six flat blades with radially tapered widths. The corresponding closed impeller, 6RTW-FCI, provided a flow path with a radially decreased cross-sectional area. Because the volumetric flow rate inside the closed impeller remains almost constant radially, the narrow-

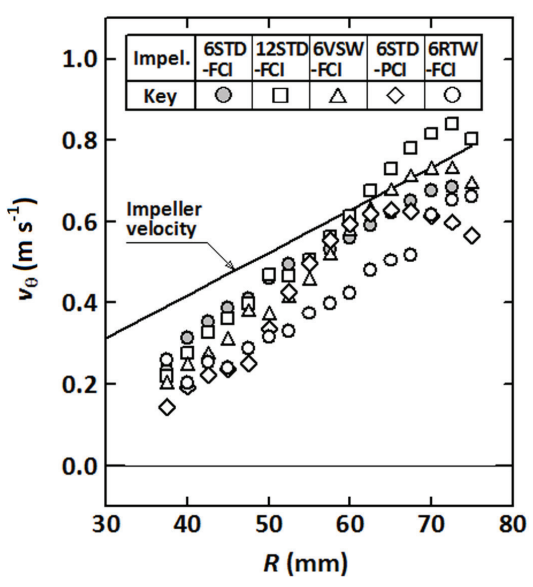


Fig. 2 (a) – Changes in average circumferential velocity, $v_{o'}$ as viewed from radial position, R, in liquid flows produced by the closed impellers

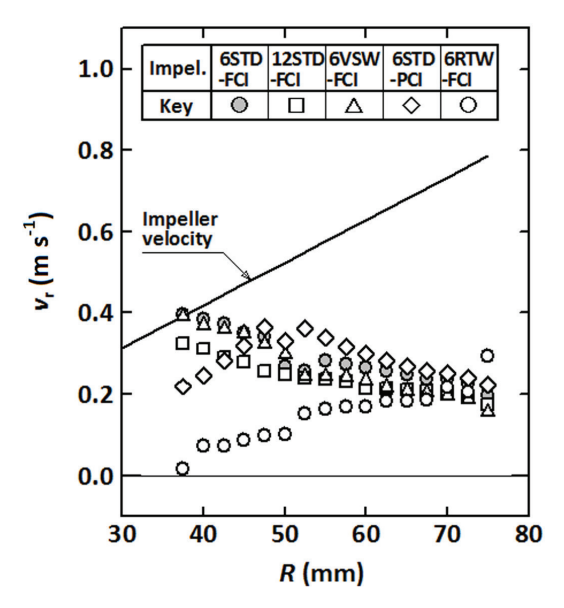


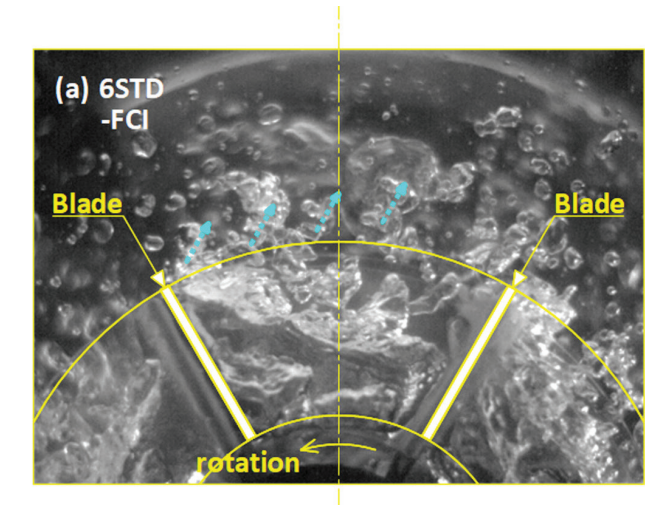
Fig. 2 (b) – Changes in average radial velocity, v, as viewed from radial position, R, in liquid flows produced by the closed impellers

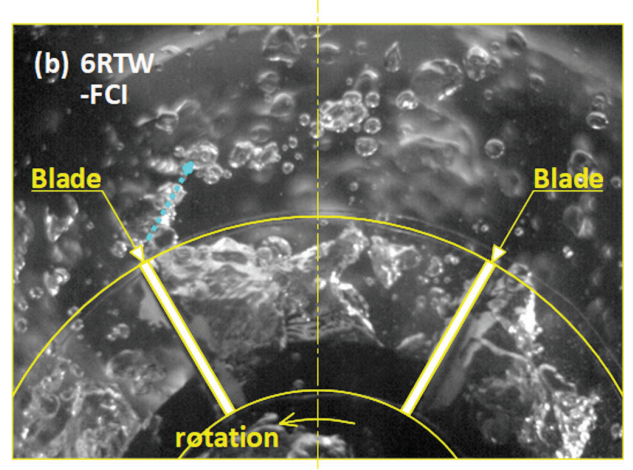
ing of the flow path induces an accelerated flow, generating a favorable pressure gradient.

The averaged circumferential and radial flow velocities, v_{θ} and v_{r} , for the 6RTW-FCI, are added to Figs. 2 (a) and (b), respectively. The v_{θ} values in the radial positions were comparable to those of the other closed impellers, while v_{r} values, though smaller overall, increased radially outward as expected. The flow pattern near the disk for the 6RTW-FCI is illustrated in Fig. 1(e). The redesigned blades yielded a more uniform internal flow, with no significant stagnant regions observed throughout the impeller rotation region, regardless of axial position.

Application of closed impellers to gas-liquid agitation

The closed impeller, designed as previously described, was applied to gas-liquid agitation. Fig. 3 shows the region where the impeller rotates at a rate, N_r , of 100 rpm under gassing at a superficial gas velocity, V_s , of 0.47 cm s⁻¹. In the Fig. 3, (a) corresponds to 6STD-FCI, (b) corresponds to 6RTW-FCI, and (c) to the original open impeller,





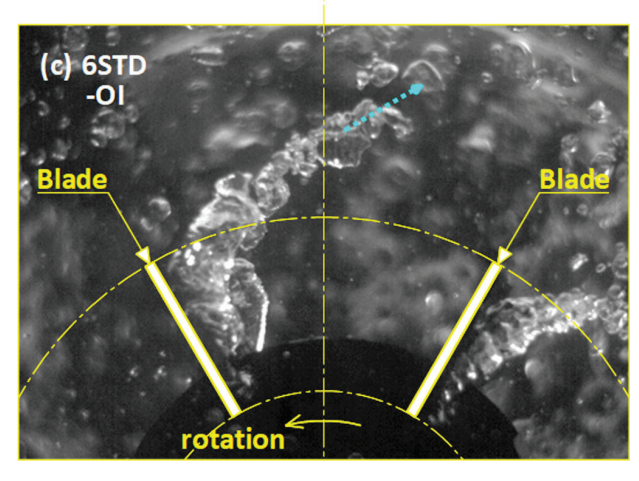


Fig. 3 – Gas behaviors in rotation regions of (a) 6STD-FCI, (b) 6RTW-FCI, and (c) 6STD-OI: dashed lines represent gas bubble generation

6STD-OI. An aeration number $(=Q/ND^3)$ of 0.059 indicates that the agitation level exceeded the aeration level²⁵. Under such aeration-agitation rate conditions, the 6STD-OI generated vortex cavities on the rear sides near the upper and lower edges of the impeller blades²⁶. These cavities capture the sparged gas and generate gas bubbles from their tails in the bulk liquid²⁷. The 6STD-FCI—with its upper and lower blade edges shrouded—did not produce vortex cavities as observed in the 6STD-OI¹⁶. Instead, the sparged gas aggregated as circumferentially elongated cavities on the rear sides of the blades near the impeller disk. Gas bubbles were released radially outward around the exit of the impeller rotation region. The internal cavities formed in 6RTW-FCI were similar to those formed in 6STD-FCI. Gas dispersion occurred around the blade tips, and gas bubbles were discharged radially into the liquid. This enhanced generation of gas bubbles through the cavities in the 6RTW-FCI can be attributed to the accelerated liquid discharge through the radially narrowed flow path. Because little flow stagnation occurred behind the blades, the gas flow within the cavities appeared to intensify toward the blade tips. Furthermore, the circumferentially stronger liquid shear flow around the blade tips may have contributed to the formation of smaller gas bubbles, similar to the action in cyclone reactors^{28,29}.

Gassed power characteristics of closed impellers

The formation of gas cavities behind the impeller blades and their dispersion as gas bubbles within the vessel were assessed based on energy considerations²⁶, expressed by the ratio of gassed to ungassed power consumption of the impeller, P_{mg}/P_{m0} . Changes in $P_{\rm mg}/P_{\rm m0}$ were observed with variation of the superficial gas velocity, $V_{\rm s}$, under a constant impeller rotation rate, $N_{\rm r}$. Fig. 4 shows the relationships between $P_{\rm mg}/P_{\rm m0}$ and $V_{\rm s}$ for 6STD-FCI and 6RTW-FCI, along with that for the original open impeller, 6STD-OI. When the impellers were operated at a rotation rate of 200 rpm, the power consumption exhibited lower values due to gassing, but the manner in which the $P_{\rm mg}/P_{\rm m0}$ changed differed among the impellers, notably between the FCIs and OI. The 6STD-OI had relatively greater decreases in the range of lower V_s values, probably because of the growth of large cavities^{3,25}. Subsequently, with increased V_{\circ} , an increase was observed as marked in the figure, suggesting impeller flooding with the formation of ragged cavities^{3,25}. Under flooding conditions—where sparged gas flushes axially across the impeller region—upward gas movement dominates the liquid flow, and gas bubbles are poorly dispersed in the bulk liquid, as reported in the literatures^{3,25}. Consequently, $P_{\rm mg}/P_{\rm m0}$ changes abruptly. For the FCIs, the decrease in $P_{\rm mg}/P_{\rm m0}$ was

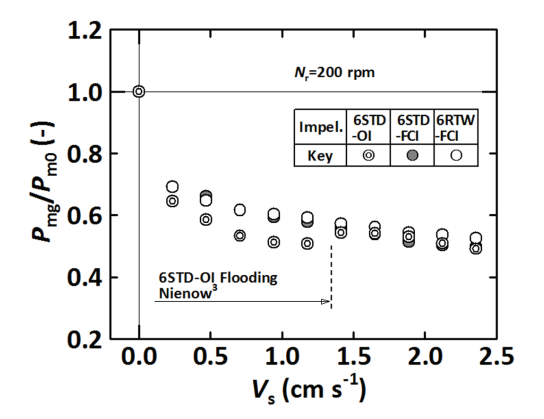


Fig. 4 – Relationships between relative gassed power consumption and superficial gas velocity for 6STD-FCI, 6RTW-FCI, and 6STD-OI

gradual and monotonic, with no subsequent increase. Within this range of gassing rates, the FCIs were presumed to remain below flooding conditions but up to the loading conditions where the sparged gas is effectively dispersed through the impeller, but unevenly distributed within the vessel^{3,25}. An additional benefit of the FCI impeller structure is that the shrouds prevent sparged gas from flushing axially through the impeller region. Consequently, the flow behavior of the gas-liquid mixture in the FCI region is probably less sensitive to increasing gassing rates. This behavior suggests that the gas condition exerts a smaller effect on the internal liquid flow pattern related to the cavity configuration. For the FCIs, the relationships between $P_{\rm mg}/P_{\rm m0}$ and $V_{\rm s}$ are shown in Fig. 5 with the impeller rotation rate, N_r , as a parameter. Gradual and monotonic decreases in the respective FCIs were common for the various N_{i} values, indicating that the cavities formed in the FCIs were stable, regardless of the agitation conditions. Therefore, FCIs can achieve effective gas-liquid agitation at various aeration-agitation rates.

The ungassed power consumption of the impellers is represented by the power number $[N_{p0}=P_{m0}/(\rho N_{\rm i}^3D_{\rm i}^5)]$. The values were 4.8, 3.7 and 2.4 for the 6STD-OI, 6STD-FCI, and 6RTW-FCI, respectively. The N_{p0} values for the FCIs were lower than that for the OI, which was attributed to the absence of a trailing vortex because of the shrouded blades of the impeller. This is considered the basis for FCI agitation vessels with reduced shearing action.

Gas-liquid dispersions by closed impellers

Fig. 6 shows the gas-liquid conditions within the vessels agitated by the 6STD-FCI, 6RTW-FCI, and 6STD-OI, respectively. Under the given aeration-agitation conditions ($N_r = 150$ rpm, $V_s = 1.41$ cm s⁻¹), the 6STD-OI experienced flooding by the sparged gas^{3,25}. In contrast, the FCIs appeared to maintain

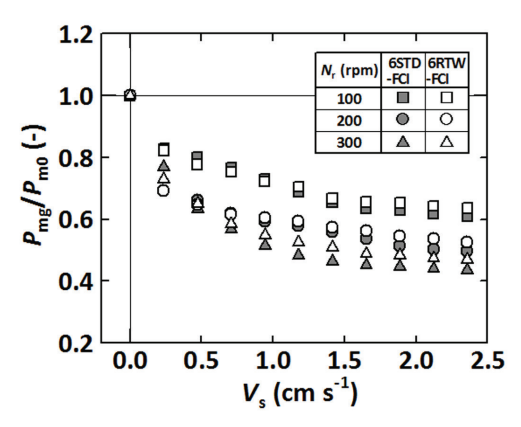


Fig. 5 – Relationships between relative gassed power consumption and superficial gas velocity for the closed impellers rotating at different rates

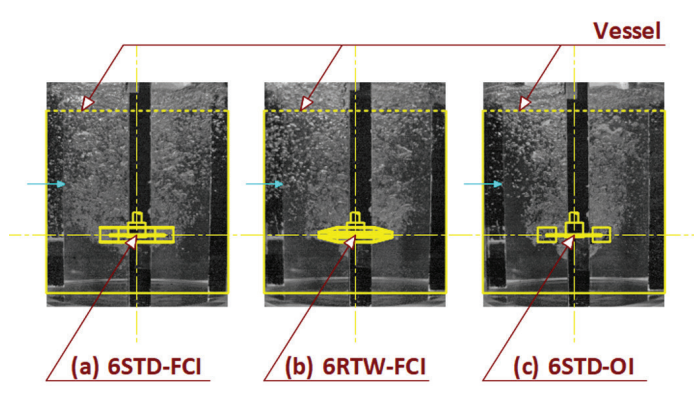


Fig. 6 – Gas-liquid dispersions within vessels agitated by (a) 6STD-FCI, (b) 6RTW-FCI, and (c) 6STD-OI

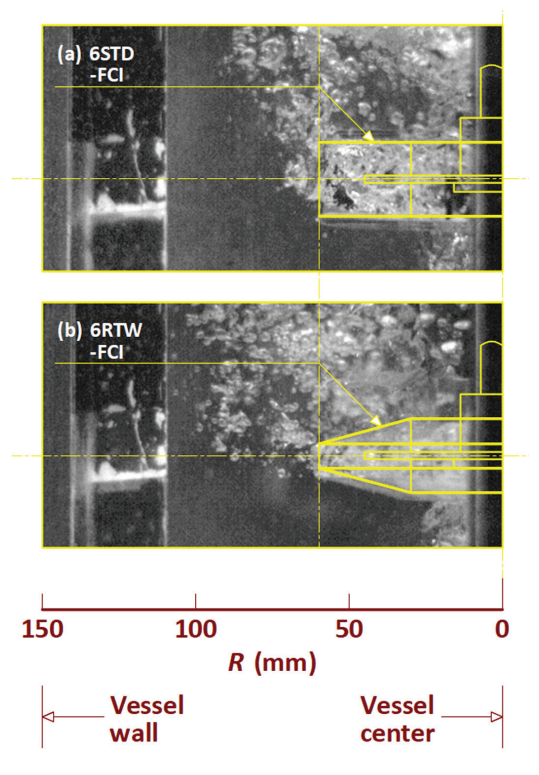


Fig. 7 – Discharges of gas-liquid mixture performed by the closed impellers

their inherent radial discharge action to some extent for both gas bubbles and liquid. A difference in gas bubble distribution was observed in the region of the vessel wall side, as indicated by the arrows in the figures. Fig. 7 compares, in photographic form, the discharge regions of the gas-liquid mixture between the FCIs. The rotation rates were adjusted so that both impellers consumed the same amount of ungassed power. At $V_s = 0.94$ cm s⁻¹, the N_s values were 100 rpm for the 6STD-FCI and 116 rpm for the 6RTW-FCI. Although gas capture and the resulting gas retention in the impeller region appeared to be superior in the 6STD-FCI, the 6RTW-FCI, exhibited a more pronounced discharge of gas bubbles. The 6RTW-FCI, developed here as a closed impeller, was characterized by effective energy conversion from pressure head to velocity head, resulting in enhanced gas bubble generation and discharge. It has been noted that the gas-liquid flow behavior differed between direct and indirect impeller loading of sparged gas³⁰⁻³². A strong liquid flow produced by the impeller promotes gas recirculation into the impeller region, leading to favorable gasliquid dispersion. For the 6RTW-FCI, which features superior discharge performance and structural shrouding, this indirect loading effect is expected to further enhance gas-liquid dispersion.

Conclusion

The previously developed closed impeller (6STD-FCI) was modified by adjusting the dimensions of the flow path between neighboring blades. An impeller with twelve flat blades of standard width and an impeller with six flat blades of vertically small width were employed as the original designs for closed impellers (12STD-FCI and 6VSW-FCI). In addition, a standard turbine-type impeller was partially closed (6STD-PCI).

Investigations of the internal liquid flow in these closed impellers highlighted the significance of radial flow velocity in optimizing closed-impeller design. Based on these findings, a new impeller with six flat blades of radially tapered width was developed for closed-mode operation. This closed impeller (6RTW-FCI), produced an accelerated radial flow within the flow path, improving the internal flow uniformity and eliminating stagnant regions.

The 6RTW-FCI was then applied to gas-liquid agitation, and the flow behavior of the gas-liquid mixture was examined through flow visualization and measurement. Internal cavities formed within the 6RTW-FCI generated gas bubbles radially outward around the tips of the impeller blades. The ratio of gassed to ungassed power consumption of the impeller reflected the formation of gas cavities and

their dispersion as gas bubbles. Across a range of aeration-agitation rates, the 6RTW-FCI demonstrated superior discharge performance and characteristic energy conversion to that of the 6STD-FCI, resulting in favorable gas-liquid dispersion.

Nomenclature

 D_i – impeller diameter, mm

D. – vessel diameter, mm

 N_{p0} – ungassed impeller power number, –

 N_r – impeller rotation rate, rpm

 $P_{\rm m0}$ – ungassed impeller power consumption, W

P_{ma} – gassed impeller power consumption, W

Q - volumetric gas flow rate, L min⁻¹

R - radial distance from vessel center, mm

 V_{\perp} – superficial gas velocity, cm s⁻¹

v_r - radial velocity component of liquid flow, m s⁻¹

 $v_{\rm \theta}$ - circumferential velocity component of liquid flow, m s⁻¹

 ρ – liquid density, kg m⁻³

References

- Garcia-Ochoa, F., Gomez, E., Bioreactor scale-up and oxygen transfer rate in microbial processes: An overview, Biotechnol. Adv. 27 (2009) 153. doi: https://doi.org/10.1016/j.biotechadv.2008.10.006
- Scargiali, F., Busciglio, A., Grisafi, F., Brucato, A., Mass transfer and hydrodynamic characteristics of unbaffled stirred bio-reactors: Influence of impeller design, Biochem. Eng. J. 82 (2014) 41. doi: https://doi.org/10.1016/j.bej.2013.11.009
- 3. *Nienow, A. W.*, Hydrodynamics of stirred bioreactors, Appl. Mech. Rev. **51** (1998) 3. doi: https://doi.org/10.1115/1.3098990
- Gebousky, O., Idzakovicova, K., Haidl, J., Mixing characteristics of unbaffled bioreactor with levitating radial impeller, Chem. Eng. Sci. 276 (2023) 118801. doi: https://doi.org/10.1016/j.ces.2023.118801
- 5. Ayazi Shamlou, P., Makagiansar, H. Y., Ison, A. P., Lilly, M. D., Thomas, C. R., Turbulent breakage of filamentous microorganisms in submerged culture in mechanically stirred bioreactors, Chem. Eng. Sci. 49 (1994) 2621. doi: https://doi.org/10.1016/0009-2509(94)E0079-6
- Khalili, F., Jafari Nasr, M. R., Ein-Mozaffari, F., Soltaniye, M., Investigation of the gas-liquid flow in an agitated vessel equipped with an ASI impeller by using tomography method, Iran. J. Chem. Chem. Eng. 39 (2020) 321. doi: https://doi.org/10.30492/ijcce.2019.37427
- 7. Manickavasagam, V. M., Anupindi, K., Bhatt, N., Srivastava, S., Characterizing the effect of impeller design in plant cell fermentations using CFD modeling, Sci. Rep. 15 (2025) 9322276. doi: https://doi.org/10.1038/s41598-025-92385-y
- 8. Sanchez Perez, J. A., Rodriguez Porcel, E. M., Casas Lopez, J. L., Fernandez Sevilla, J. M., Chisti, Y., Shear rate in stirred tank and bubble column bioreactors, Chem. Eng. J. 124 (2006) 1.

doi: https://doi.org/10.1016/j.cej.2006.07.002

- Mohseni, S., Khoshfetrat, A. B., Rahbarghazi, R., Khodabakhshaghdam, S., Kaleybar, L. S., Influence of shear force on ex vivo expansion of hematopoietic model cells in a stirred tank bioreactor, J. Biol. Eng. 17 (2023) 38. doi: https://doi.org/10.1186/s13036-023-00358-4
- Bustamante, M. C. C., Cerri, M. O., Badino, A. C., Comparison between average shear rates in conventional bioreactor with Rushton and Elephant ear impellers, Chem. Eng. Sci. 90 (2013) 92. doi: https://doi.org/10.1016/j.ces.2012.12.028
- Berry, J. D., Liovic, P., Sutalo, I. D., Stewart, R. L., Glattauer, V., Meagher, L., Characterisation of stresses on microcarriers in a stirred bioreactor, Appl. Math. Model. 40 (2016) 6787.
 doi: https://doi.org/10.1016/j.apm.2016.02.025
- 12. Wyrobnik, T. A., Oh, S., Ducci, A., Micheletti, M., Engineering characterization of the novel Bach impeller for bioprocessing applications requiring low power inputs, Chem. Eng. Sci. 252 (2022) 117263. doi: https://doi.org/10.1016/j.ces.2021.117263
- Rahimzadeh, A., Ein-Mozaffari, F., Lohi, A., Analyzing of hydrodynamic stress and mass transfer requirements of a fermentation process carried out in a coaxial bioreactor: A scale-up study, Bioprocess Biosystems Eng. 47 (2024) 633. doi: https://doi.org/10.1007/s00449-024-02990-w
- Pincovschi, I., Dragomirescu, A., Modrogan, C., Influence of impeller design on oxygen transfer in a stirred water tank with square cross-section, Biochem. Eng. J. 216 (2025) 109649.
 - doi: https://doi.org/10.1016/j.bej.2025.109649
- Yoshida, M., Ebina, H., Ishioka, K., Oiso, K., Shirosaki, H., Tateshita, R., Hydraulic design and power characterization of closed turbine-type agitator, Int. J. Chem. Reactor Eng. 15 (2017) 20160198. doi: https://doi.org/10.1515/ijcre-2016-0198
- Yoshida, M., Kosaka, T., Mukai, Y., Nakahara, K., Kiyota, R., Gas-liquid dispersion agitated by closed turbine type impeller, Chem. Ind. Chem. Eng. Q. 31 (2025) 193. doi: https://doi.org/10.2298/CICEQ240411027Y
- 17. Brun, K., Kurz, R., Analysis of secondary flows in centrifugal impellers, Int. J. Rotating Machinery 1 (2005) 45. doi: https://doi.org/10.1155/IJRM.2005.45
- Li, X., Chen, B., Luo, X., Zhu, Z., Effects of flow pattern on hydraulic performance and energy conversion characterisation in a centrifugal pump, Renew. Energy 151 (2020) 475. doi: https://doi.org/10.1016/j.renene.2019.11.049
- Li, X., Chen, H., Chen, B., Luo, X., Yang, B., Zhu, Z., Investigation of flow pattern and hydraulic performance of a centrifugal pump impeller through the PIV method, Renew. Energy 162 (2020) 561.
 doi: https://doi.org/10.1016/j.renene.2020.08.103
- 20. Chen, W., Li, Y., Liu, Z., Hong, Y., Understanding of energy conversion and losses in a centrifugal pump impeller, Energy 263 (2023) 125787. doi: https://doi.org/10.1016/j.energy.2022.125787

- Fonseca, W. D. P., Perissinotto, R. M., Cerqueira, R. F. L., Verde, W. M., Castro, M. S., Franklin, E. M., Particle image velocimetry in the impeller of a centrifugal pump: Relationship between turbulent flow and energy loss, Flow Meas. Instrum. 99 (2024) 102675. doi: https://doi.org/10.1016/j.flowmeasinst.2024.102675
- 22. Liu, X. D., Li, Y. J., Liu, Z. Q., Yang, W., Experimental and numerical investigation of stall mechanism in centrifugal pump impeller, J. Appl. Fluid Mech. 15 (2022) 927. doi: https://doi.org/10.47176/jafm.15.03.33165
- 23. Wu, C., Pu, K., Li, C., Wu, P., Huang, B., Wu, D., Blade redesign based on secondary flow suppression to improve energy efficiency of a centrifugal pump, Energy **246** (2022) 123394.
 - doi: https://doi.org/10.1016/j.energy.2022.123394
- 24. Cheah, K. W., Lee, T. S., Winoto, S. H., Numerical study of inlet and impeller flow structures in centrifugal pump at design and off-design points, Int. J. Fluid Machinery Systems 4 (2011) 25. doi: https://doi.org/10.5293/IJFMS.2011.4.1.025
- 25. *Middleton, J. C.*, Gas-liquid dispersion and mixing, in Harnby, N., Edwards, M. F. and Nienow A. W. (Eds.), Mixing in the process industries, Butterworth-Heinemann, Oxford, 1992, pp 322-363.
- Bruijn, W., van't Riet, K., Smith, J. M., Power consumption with aerated Rushton turbines, Trans. Inst. Chem. Engrs. 52 (1974) 88.
- 27. van't Riet, K., Smith, J. M., The behaviour of gas-liquid mixtures near Rushton turbine blades, Chem. Eng. Sci. 28 (1973) 1031. doi: https://doi.org/10.1016/0009-2509(73)80005-3
- 28. Zhang, M., Chen, J., Tang, M., Liu, X., Song, Y., Zhang, H., Wang, Z., Visualization investigation of dispersed phase droplet formation regimes in a circumferential shear flow composed of immiscible liquid, J. Braz. Soc. Mech. Sci. Eng. 45 (2023) 62. doi: https://doi.org/10.1007/s40430-022-03960-7
- 29. Zhang, M., Chen, J., Liu, X., Xiao, X., Zhang, H., Wang, Z., Zhang, L., Experimental study on the dispersed phase droplet formation process in a circumferential shear flow in dripping regime, Chem. Eng. Res. Des. 189 (2023) 583. doi: https://doi.org/10.1016/j.cherd.2022.11.024
- 30. Pandit, A. B., Rielly, C. D., Niranjan, K., Davidson, J. F., The convex bladed mixed flow impeller: A multipurpose agitator, Chem. Eng. Sci. 44 (1989) 2463. doi: https://doi.org/10.1016/0009-2509(89)85190-5
- Sardeing, R., Aubin, J., Xuereb, C., Gas-liquid mass transfer, a comparison of down- and up-pumping axial flow impellers with radial impellers, Chem. Eng. Res. Des. 82 (2004) 1589.
 doi: https://doi.org/10.1205/cerd.82.12.1589.58030
- 32. Bakker, A., Van den Akker, H. E. A., Gas-liquid contacting with axial flow impellers, Chem. Eng. Res. Des. 72 (1994) 573. doi: https://doi.org/10.1016/0263-8762(94)00037-M